EFFECT OF SONICATION ON NUCLEOTIDE-DEPENDENT LIGHT SCATTERING CHANGES IN RETINAL ROD OUTER SEGMENT SUSPENSIONS

J. W. LEWIS, L. E. SCHAECHTER, E. A. DRATZ, AND D. S. KLIGER
Department of Chemistry, University of California at Santa Cruz, Santa Cruz, California 95064

ABSTRACT Near-infrared light scattering from suspensions of rod outer segment fragments is a useful probe of visible-light–activated changes in peripheral membrane proteins in photoreceptor cells. Limited sonication of suspensions has been shown to increase the amplitude of light induced turbidity changes in the presence of guanosine triphosphate by a factor of 2. Further sonication led to a decrease in the signal amplitude by an order of magnitude. This reduction has been puzzling, since the activity of the GTP-binding protein (as measured by GTP hydrolysis turnover number) was unaffected by the range of sonication used. This effect of sonication is investigated here using a novel, Reticon-based apparatus that measures the angular distribution of scattered light from samples as small as 1 μl. The results show that even at high rhodopsin concentrations (125 μM) with millimeter path lengths, significant amounts of unscattered light are transmitted by the samples. A simple phenomenological theory that assumes a constant fractional change in scattering power (15%), independent of amount of sonication, explains the effect of sonication on the angle dependence data as well as the original turbidity data. The results have general relevance for optimization of light-scattering studies of membrane systems.

INTRODUCTION

It has been shown that near-infrared light scattering from retinal rod outer segment (ROS) suspensions provides useful information about light-activated enzymatic processes in photoreceptors (Bignetti et al., 1980; Kuhn et al., 1981; Bennett and Dupont, 1985; Caretta and Stein, 1985). We recently reported that limited sonication of ROS suspensions could be used to increase the amplitude (and hence the sensitivity) of the light-induced scattering changes (Lewis et al., 1984). Further sonication led to decreases in the signal amplitude by an order of magnitude (see Fig. 1). This reduction was puzzling because the light-induced enzyme activity (as measured by substrate turnover number) appeared to be unaffected by the range of sonication used. Sonication thus seemed principally to modulate the expression of enzymatic activities as light-scattering changes.

Besides its significance as a method to improve the sensitivity of light-scattering as a probe of enzymatic changes, it is important to understand the effects of sonication for other reasons. The plasma membrane at the outer surface of the ROS is damaged to varying degrees in ROS preparations. Since there is much current interest in processes that involve the disk membrane vesicles interior to the ROS, the presence of intact plasma membranes can present problems. Several methods have been used which are intended to destroy the osmotic integrity of the plasma membranes (Schnetkamp et al., 1979; Uhl et al., 1977; Kuhn et al., 1981; Caretta and Stein, 1985). Of these, sonication is the most effective at both disrupting the plasma membranes and improving optical quality of samples. Study of sonication is also interesting because the mechanism of coupling between biochemical events and light-scattering changes in ROS suspensions, although poorly understood at present, seems to involve changes in size of particle aggregates (Lewis et al., 1984; Caretta and Stein, 1985).

To investigate the effects of sonication, we measured the angular distribution of scattered light from sonicated ROS suspensions. For this purpose, a novel apparatus based on a Reticon photodiode array was developed that measures simultaneously the time and angle dependence of scattered light from a sample volume of 1 μl. Interpretation of the results using a simple phenomenological theory explains the effect of sonication on ROS signal amplitudes and gives useful insight for optimization of light-scattering measurements made in other systems such as chloroplast thylakoid membranes.

METHODS

The work reported here was carried out using two completely independent apparatuses. One, the turbidity apparatus, had the advantages of sensitiv-

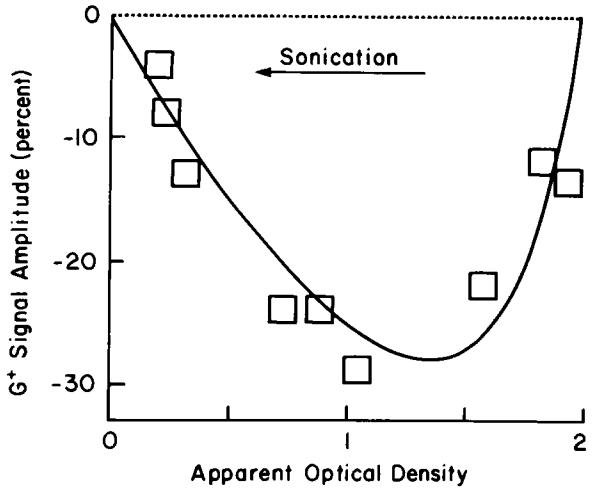

FIGURE 1 G^+ signal amplitude vs. sonication. Samples of ROS suspension were sonicated to varying degrees and the apparent optical density at 730 nm was measured in the turbidity apparatus. The maximum change in transmittance during the G^+ signal was then measured. The curve is a fit to the data using the model described in the text which accounts for the presence of both scattered and transmitted light at 0°. A scattering change of 15%, independent of sonication, fits all points. The maximum amplitude of the G^+ signal was obtained with 30 s of sonication.

ity and convenience of use. The other, the angle dependence apparatus, had the advantage of providing the additional information needed to explain the effects of sonication observed in the first apparatus.

Measurements of the photolysis-induced turbidity increase in the presence of guanosine triphosphate (GTP), the G^+ signal, were made using a turbidity apparatus similar to the one described previously (Lewis et al., 1984). Changes in this apparatus included use of a small photoflash as a bleaching source and collection of scattered light over a cone of slightly larger angle (10°) about the monitoring beam axis. Neutral density filters were used to attenuate the actinic flash so that it bleached ~2% of the rhodopsin in a sample whose apparent optical density was 1. A bleach of this size is 200-fold larger than needed to saturate the G^+ signal.

Angle dependence of the transmitted and scattered light was measured using the apparatus shown in Fig. 2. Data was collected from the Reticon using a microcomputer with an analog-to-digital converter. The diode array output was recorded every 100 ms. Signals from 16 channel groups, or angular segments, were summed. This was done both to reduce the amount of data to be stored and because the sample subtended an angle of

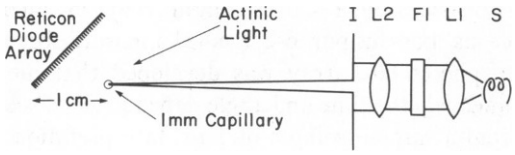

FIGURE 2 Overhead view of apparatus to measure angle dependence of transmitted and scattered light. Light from a tungsten halogen source, S, was collimated by lens L1 and passed through a 730-nm interference filter and then focused in the sample by the achromatic lens L2. The sample is held in a 1-mm inside diameter glass capillary that was oriented perpendicular to the plane of the monitoring beam and the diode array. The iris, I, was adjusted to give a beam whose angular spread was 2°. Transmitted and scattered light was detected by a Reticon 512G linear photodiode array with 512, 25 μm square elements. The array was oriented at 45° to the monitoring beam.

approximately 6° as viewed from each detector element and thus already convoluted the signals from a small range of angles. The choice of a 512 element array was based on the need to collect light over an angular range of approximately 90°.

Bovine ROS were prepared and sonicated as previously described (Lewis et al., 1984). For all experiments, ROS suspensions contained 5 mg/ml rhodopsin in buffer (10 mM TRIS.HCl,100 mM NaCl,1mM $MgCl_2$,1 mM dithiothreitol, pH 7.3). Shortly before photolysis, 160 μM GTP and 16 μM adenosine triphosphate (ATP) were added to samples. ATP was included so that any traces of bleached rhodopsin would be inactivated (Sitaramayya and Liebman, 1983). Samples of 10 μL were loaded into the capillary cell of the angle dependence apparatus by expelling them from an Eppendorf pipette through Tygon tubing attached to the capillary. After delivery, the tubing was closed with a pinch clamp. Sample loading was done in total darkness.

RESULTS AND DISCUSSION

The original hypothesis pursued here was that sonication changes the G^+ signal amplitude (Fig. 1) by moving angular nodes in the scattering difference pattern (scattering after photolysis minus scattering before photolysis). These nodes result from the fact that after photolysis more light is scattered at some angles and less at others. Since the signal observed in the turbidity apparatus is the average over approximately 10° about the monitoring beam axis, shifting the position of an angular node within that 10° range could dramatically affect the detected amplitude.

To test this hypothesis, the angle dependence of the photolysis induced light scattering changes was measured for samples sonicated from 15 s to 2 min. Representative data is shown in Fig. 3. In the first angular segment, from 0° to 1.7°, (curve *A*) the characteristic G^+ signal seen previously is observed and persists until the added GTP is hydrolysed. As can be seen, a node in the scattering difference occurs in angular segment 2, from 1.7° to 3.4° (curve *B*). For the next few angular segments, photolysis induces an increase in scattering that complements the G^+ signal. The slope in curve *B* gives some evidence that after photolysis the node moves slightly outward within angular

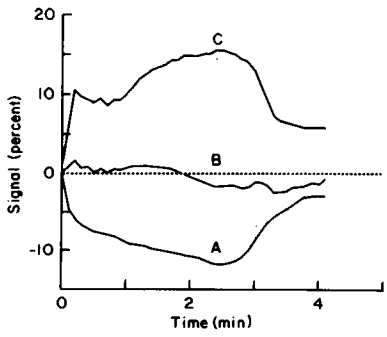

FIGURE 3 Time course of the G^+ signal at three angle segments near 0°. Curve *A* is the signal observed at the first angular segment (16 channels, 0 to 1.7°) on the Reticon detector. *B* and *C* are the signals observed in the second and third angular segments, 1.7°–3.4° and 3.4°–5.1°, respectively. The sample used here corresponds to the point in Fig. 1 with apparent optical density 0.7.

segment 2 while GTP hydrolysis occurs. This has the same time course as, and possibly accounts for, the downward slope in curve A that follows the initial, more rapid phase of the G^+ signal. Data for other levels of sonication were qualitatively the same. The amplitude of the observed scattering changes was affected by sonication. However, for all sonications the angle dependence was similar, in that the node in the scattering difference pattern was confined to angular segment 2, from 1.7° to 3.4°. We conclude from the angle dependence data that while the changing position of a node may cause the ramp shaped bottom of the G^+ signal, it cannot account for the effect of sonication on G^+ amplitude.

The effect of sonication on the G^+ signal amplitude becomes clearer when the angular distribution of scattered light before photolysis is considered. Data for four levels of sonication are plotted in Fig. 4. Consideration of these results shows that for even the least sonicated sample, a measureable amount of transmitted (unscattered) light is present at 0°. To separate the transmitted intensity, I, from the total intensity detected at 0°, $I_{\text{Total}}(0)$, we extrapolate, as shown in the inset to Fig. 4, the scattered energy (from angular segments greater than two, where no transmitted light is present) to obtain a value of the scattered intensity at 0°, $I_S(0)$. This allows separation of transmitted intensity, I, from the total intensity detected at 0° since $I_{\text{Total}}(0) = I + I_S(0)$.

The presence of significant transmitted intensity at 0° suggests that the effect of sonication on the G^+ signal may arise from varying the proportion of transmitted light rather than from varying the amplitude of the photolysis-induced scattering change. We hypothesize, then, that the G^+ signal is a fixed, fractional change in the scattering power of the membrane vesicle aggregates. For strongly scattering particles, $I_S(0) >> I$ and any change in I due to a fractional increase in scattering is small compared with $I_S(0)$. For more weakly scattering particles, such that $I_S(0) \sim I$, a comparatively small change in the scattering power can cause a relatively large change in I. Since I is approximately 50% of the signal, this leads to a large change in signal. For weakly scattering particles, $I_S(0) << I$, and I is large compared with any fraction of the scattered light. Here again small signals result.

To model this effect, consider the transmitted intensity to follow an exponential law (van de Hulst, 1957)

$$I = I_0 e^{-\gamma l}. \tag{1}$$

Of the light scattered from the beam, some fraction, P_0, is forward scattered into the angular segment at 0°, so

$$I_S(0) = P_0 I_0 (1 - e^{-\gamma l}). \tag{2}$$

The detector sees the sum of I and $I_S(0)$ so if γ increases by a fraction k, the fractional change, S, in the signal is given by

$$S = \frac{\Delta I_{\text{Total}}(0)}{I_{\text{Total}}(0)} = \frac{e^{-\gamma(1+k)l}(1 - P_0) + P_0}{e^{-\gamma l}(1 - P_0) + P_0} - 1. \tag{3}$$

P_0 can be estimated for the data from Fig. 4 as shown in the inset by drawing a right triangle with one vertex at angle segment 20 and whose hypotenuse fits the points at angle segments 3–20 (angle segments 1 and 2 contain contributions from transmitted light). Since all the triangles so defined have the same base, and since P_0 is the ratio of the height of the triangle to the area of the triangle, P_0 assumes a uniform value of 0.1. The fractional scattering change, k, can then be adjusted to fit the amplitude of the scattering change at 0°. A fractional scattering change of 15% fits the data well for all sonications as shown by Fig. 5. From this result it appears that the underlying physical process, the fractional change in scattering, is not affected by the amounts of sonication used here.

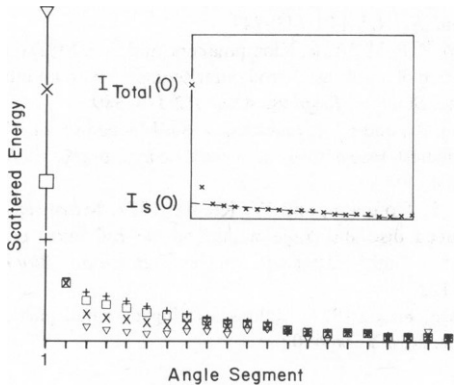

FIGURE 4 Angular dependence of total light scattered before photolysis. The intensity detected in each angular segment was multiplied by the total area of the conic section at that angle to obtain the total energy scattered at each angle. The symbols +, □, x, and ▽ represent sonications of 15, 30, 60, and 120 seconds and correspond to the samples at 1.6, 1.1, 0.7, and 0.3 apparent optical density in Fig. 1. I_0 was the same for all samples. The inset shows how the light scattered at 0°, $I_S(0)$ is estimated from the angle dependence data (see text).

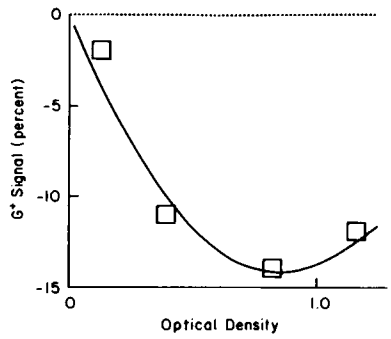

FIGURE 5 G^+ Signal amplitude vs. sonication as measured in the angle dependence apparatus. Samples of ROS suspensions were sonicated to varying degrees. The actual optical density was measured by extrapolating the scattered light shown in Fig. 4 to 0°, so that true transmitted light could be estimated. The amplitude of the G^+ signal was measured at 0°. The curve is the fit to the data for a 15% scattering change and with no other adjustable parameters.

The same model can be used to fit the data from the 2 mm path length turbidity apparatus. Since this apparatus provides no angle dependence information, some other basis must be used to estimate P_0. At low values of apparent optical density, the value 0.1 obviously remains appropriate. At the higher optical densities obtained using the longer path length cell and photomultiplier detector of the turbidity apparatus, P_0 will clearly decrease until it approaches the value expected for the probability of a randomly emerging ray striking the detector aperture. This limiting value can be estimated to be ~0.01 (by taking the ratio of the detector aperture to the area of the sphere centered on the sample that contains the detector aperture). The functional form that carries P_0 between these limits is not obvious. However, one that has the correct qualitative behavior is

$$P_0 = 0.1[1 - 0.9(1 - e^{-\gamma l})]. \quad (4)$$

Using this function for P_0, Fig. 1 shows that one can obtain a reasonable fit to the turbidity apparatus data using the same fractional scattering change as used for the angle dependence results. Here the relation

$$OD_{apparent} = -\log\{[I - I_S(0)]/I_0\} \quad (5)$$

was used to calculate the apparent optical density for the fit. Note that because of the longer path length, the signals here are roughly twice as large as for the data obtained at zero degrees using the angle dependence apparatus. In all, the simple explanation given here accounts for data taken in quite different apparatuses that yield optimal signals considerably different in amplitude and apparent optical density.

This type of explanation provides a useful framework for designing experiments to study the underlying enzymology. It says little, however, about the mechanism coupling light-scattering changes to molecular processes. Fortunately, direct microscopic examination has shown that the light scattering changes observed here are caused by membrane vesicle aggregation changes (Caretta and Stein, 1985). Such aggregates are extremely irregular in size and shape, making it difficult even with angle-dependence data to propose a unique quantitative model. The data presented here do show how light-scattering experiments can be optimized for study of the associated enzymatic processes. For such studies light-scattering proves more useful than microscopy since it provides a measurement more amenable to quantitative analysis.

In conclusion, the light scattering data can be fit by a model that assumes that sonication affects the amplitude of the G^+ signal principally by reducing the fractional amount of light scattered by the membrane vesicles in the sample, rather than by some more specific disruption of the system. Further, the G^+ signal seems to be associated with a fixed fractional change in light-scattering. To optimally detect such a change, roughly equal amounts of scattered and transmitted light should be present in the detector aperture. Sonication provides a convenient means of adjusting this ratio, while at the same time efficiently disrupting the ROS plasma membrane and improving the physical properties of the sample for optical monitoring of light-scattering changes.

This work was supported by National Institutes of Health grants EY00983 (to D. S. Kliger) and EY00175 (to E. A. Dratz).
Received for publication 22 January 1986 and in final form 3 June 1986.

REFERENCES

Bennett, N., and E. Dupont. 1985. The G-protein of retinal rod outer segments (tranducin). Mechanism of interaction with rhodopsin and nucleotides. *J. Biol. Chem.* 260:4156–4168.

Bignetti, E., A. Cavaggioni, P. Fasella, S. Ottonello, and G. L. Rossi. 1980. Light and GTP effects on the turbidity of frog visual membrane suspensions. *Mol. Cell Biochem.* 30:93–99.

Caretta A., and P. J. Stein. 1985. cGMP- and phosphodiesterase-dependent light-scattering changes in rod disk membrane vesicles: Relationship to disk vesicle-disk vesicle aggregation. *Biochemistry.* 24:5685–5692.

Kuhn, H., N. Bennett, M. Michel-Villaz, and M. Chabre. 1981. Interactions between photoexcited rhodopsin and GTP-binding protein: Kinetic and stoichiometric analyses from light-scattering changes. *Proc. Natl. Acad. Sci. USA.*78:6873–6877.

Lewis, J. W., J. L. Miller, J. Mendel-Hartvig, L. E. Schaechter, D. S. Kliger, and E. A. Dratz. 1984. Sensitive light scattering probe of enzymatic processes in retinal rod photoreceptor membranes. *Proc. Natl. Acad. Sci. USA.*81:743–747.

Schnetkamp, P. P. M., A. A. Klompmakers, and F. J. M. Daemen. 1979. The isolation of stable cattle rod outer segments with an intact plasma membrane. *Biochim. Biophys. Acta.* 552:379–389.

Sitaramayya, A., and P. A. Liebman. 1983. Mechanism of ATP quench of phosphodiesterase activation in rod disc membranes. *J. Biol. Chem.* 258:1205–1209.

Uhl, R., K. P. Hofmann, and W. Kreutz. 1977. Measurement of fast light-induced disc shrinkage within bovine rod outer segments by means of a light-scattering transient. *Biochim. Biophys. Acta.* 469:113–122.

Van de Hulst, H. C. 1957. Light scattering by small particles, Dover Publishing, New York. 470 pp.